Journal of Alloys and Compounds 507 (2010) 399–404

Contents lists available at ScienceDirect

Journal of Alloys and Compounds

journal homepage: www.elsevier.com/locate/jallcom

# Effect of substitutional Mo on diffusion and site occupation of hydrogen in the BCT monohydride phase of V–H system studied by $^1$H NMR

Kohta Asano*, Shigenobu Hayashi, Yumiko Nakamura, Etsuo Akiba

*National Institute of Advanced Industrial Science and Technology (AIST), AIST Central-5, 1-1-1, Higashi, Tsukuba, Ibaraki 305-8565, Japan*

ARTICLE INFO

*Article history:*
Received 5 July 2010
Received in revised form 2 August 2010
Accepted 4 August 2010
Available online 11 August 2010

*Keywords:*
Hydrogen storage materials
Metal hydrides
V–Mo alloys
Diffusion
Nuclear magnetic resonance (NMR)

ABSTRACT

The diffusion and site occupation of hydrogen in the monohydride phase of $V_{1-x}Mo_x$–H ($0 \le x \le 0.1$) were studied by means of $^1$H nuclear magnetic resonance (NMR). Hydrogen atoms in $VH_{0.68}$ occupied the octahedral (*O*) sites in a body centered tetragonal (BCT) structure. The addition of Mo to V reduced the activation energy for hydrogen diffusion, $E_H$, for the *O* sites. In $V_{0.9}Mo_{0.1}H_{0.68}$ hydrogen atoms occupied both the *O* and tetrahedral (*T*) sites, which was demonstrated by two components observed in the temperature dependence of the $^1$H spin-lattice relaxation time. The value of $E_H$ for the *T* sites was lower than that for the *O* sites. Hydrogen atoms in $V_{0.9}Mo_{0.1}H_{0.68}$ diffused faster than those in $VH_{0.68}$.



## 1. Introduction

Hydrogen storage vessels filled with hydrogen storage materials are one of the most realistic onboard hydrogen storage systems for fuel cell vehicles [1–4]. V based and Ti based alloys which have a body centered cubic (BCC) structure are attractive hydrogen storage materials because the hydrogen content in high pressure metal hydride (MH) vessels using the BCC alloys is 2.5 times higher on a volume basis than that of compressed gas vessels under a hydrogen pressure of 35 MPa [4]. For more than 10 years, we have developed BCC alloys for onboard hydrogen storage and the alloys consisted of Ti, V, Cr and Mn have been synthesized from the concept 'Laves phase related BCC solid solution' [5,6].

The high pressure MH vessels are required to supply hydrogen to the fuel cells even in cold climates. The heat of formation of the hydride phase has a linear relation with the equilibrium hydrogen pressures for formation and dissociation of the hydride phase. The dissociation pressure should be at least 0.1 MPa for the supply of hydrogen. The reduction in the heat of formation corresponds to the increase in the dissociation pressure at a given temperature. This leads to a smaller heat exchange between MH and a heat exchanger in the high pressure MH vessel during hydrogen absorption and desorption, which is preferable for heat management of the system [7,8]. One of the methods to reduce the heat of formation of the hydride phase is addition of some metal elements to the alloys. It has been reported that addition of Mo to the BCC alloys is effective to increase the dissociation pressure of their hydride phases at a given temperature [7–12]. Mo addition increased unit cell volume of the BCC lattice but decreased the radius of the interstitial site for hydrogen atoms in the lattice [11]. In consequence the stability of the hydride phase was lowered by addition of Mo.

In the phase equilibrium of the V–$H_2$ system at ambient temperatures [13], V metal with a BCC structure forms the hydrogen solid solution phase with a BCC structure (α phase), the monohydride phase with a body centered tetragonal (BCT) structure (β phase) and the dihydride phase with a face centered cubic (FCC) structure (γ phase) by hydrogenation. Hydrogen atoms occupy tetrahedral (*T*) sites in the α and γ phases and octahedral (*O*) sites in the β phase [13]. It is known that a majority of hydrogen atoms in the β phase occupies the *O* sites between V atoms along the *c*-axis ($O_z$ sites) [13]. Hydrogen diffusion is an important step in kinetics of hydrogenation and dehydrogenation. The diffusion of hydrogen in V has been investigated by means of Gorsky effect [14–17], electric resistivity [18,19], gas absorption [20] and permeation [21,22] methods. Those methods were applied to bulk specimens of the α phase but powder specimens of the β and γ phases were not suitable. Nuclear magnetic resonance (NMR) can measure the signal from hydrogen in metal powders. Hydrogen diffusion in the β phase of V–H by means of $^1$H NMR has been reported [23–27].

In the present work, the effect of Mo addition to V on diffusion of hydrogen in the β phase has been studied using $^1$H NMR. Mo addition possibly affects not only diffusion but also site occupation of hydrogen in the metal lattice because the stability of the hydride phase lowered [7–12]. The site occupation of hydrogen

* Corresponding author. Tel.: +81 29 861 4410; fax: +81 29 861 4410.
*E-mail address:* k.asano@aist.go.jp (K. Asano).

0925-8388/$ – see front matter © 2010 Elsevier B.V. All rights reserved.
doi:10.1016/j.jallcom.2010.08.018

in the β phase has been discussed by analyzing the temperature dependence of the spin-lattice relaxation time, $T_1$.

## 2. Experimental

Buttons of $V_{1-x}Mo_x$ ($x$ = 0.03, 0.05, 0.1) alloys were prepared by arc melting pellets of V with the purity of 99.9 mass% and Mo with the purity of 99.95 mass% under an argon atmosphere. The buttons were treated at 1673 K for 70 h under an argon atmosphere for homogenization. Chemical analysis using an EDAX Genesis2000 energy dispersive X-ray spectrometer (EDX) attached to a Hitachi S-3400N scanning electron microscope (SEM) showed that the alloys were in the nominal compositions. The oxygen contents of pure V and $V_{0.9}Mo_{0.1}$ prepared were determined to be 110 mass ppm and 900 mass ppm by a LECO TCH-600 oxygen determinator, respectively. Rigaku 2500V diffractometer with Cu Kα radiation was used for measurement of powder X-ray diffraction (XRD) patterns. The lattice parameters of the alloys and hydrides were calculated from the XRD peak positions.

$V_{1-x}Mo_x$ ($x$ = 0, 0.03, 0.05, 0.1) were set into the stainless steel tube and the tube was evacuated for 1 h at 423 K. Hydrogen absorption at room temperature and desorption at 1073 K were repeated 3 times under a hydrogen pressure of 5–8 MPa. Hydrogen gas of 7N purity was used. Afterward, the tube was evacuated for 3 h at 773 K. The $P$ (pressure)–$C$ (composition) isotherms at 243 and 303 K were measured using the volumetric method. Hydride specimens, $V_{1-x}Mo_xH_{0.68}$ ($x$ = 0, 0.03, 0.05, 0.1), were obtained by fixing the hydrogen pressure after the $P$–$C$ isotherm measurements. Powders of those hydrides were sealed into glass tubes under an argon atmosphere for the NMR measurements.

$^1$H NMR measurements were performed by Bruker mq20 and ASX200 spectrometers in the temperature range of 138–420 K. Larmor frequencies were 19.65 MHz for mq20 and 200.13 MHz for ASX200. The NMR spectra were measured with the solid echo pulse sequence ($90^\circ_x$–$\tau_1$–$90^\circ_y$–$\tau_2$–echo) at 200.13 MHz. The 90° pulse width was 1.9 μs. The values of $\tau_1$ and $\tau_2$ were set at 8.0 and 8.8 μs, respectively. The frequency scale of spectra, $\nu$, was expressed with respect to neat tetramethylsilane (TMS) by adjusting the signal of water to 4.877 ppm. $^1$H spin-lattice relaxation time, $T_1$, was determined using the inversion recovery pulse sequence (180°–$\tau$–90°) at 19.65 MHz and using the inversion recovery pulse sequence followed by the solid echo pulse sequence ($180^\circ$–$\tau$–$90^\circ_x$–$\tau_1$–$90^\circ_y$–$\tau_2$–echo) at 200.13 MHz. The $\tau$ value denotes the variable delay time. Those of $\tau_1$ and $\tau_2$ are the fixed delay times.

## 3. Analysis of $^1$H spin-lattice relaxation time, $T_1$

The $^1$H spin-lattice relaxation time, $T_1$, determined in the present work was analyzed by the Bloembergen, Purcell and Pound (BPP) equation [28] modified as follows. The detailed procedure for this analysis has been described in the previous reports [29,30].

The $T_1$ is expressed by Eq. (1):

$$(T_1)^{-1} = (T_{1d})^{-1} + (T_{1e})^{-1}, \tag{1}$$

where $T_{1d}$ is the contribution from modulation of nuclear dipolar interaction and $T_{1e}$ arises from fluctuation of hyperfine interaction between the nuclear spin and conduction electrons. The temperature dependence of $T_{1e}$ is given by Korringa relation, *i.e.*, $T_{1e}T$ = constant. The value of the Korringa constant was estimated by the fitting of $T_1$. The $T_{1d}$ value in Eq. (1) is described using the BPP equation on the assumption that the residence time describing the fluctuation of the $^1$H–$^1$H dipolar interaction, $\tau_H$, has a log-normal distribution:

$$(T_{1d})^{-1} = \int F(S)\left\{\frac{2}{3}M_{HH}\left[\frac{0.5\tau_H}{1+(0.5\omega_H\tau_H)^2}+\frac{2\tau_H}{1+(\omega_H\tau_H)^2}\right] + f_1 M_{HV}\left[\frac{0.5\tau_H}{1+\{(1-\gamma_V/\gamma_H)\omega_H\tau_H\}^2} + \frac{1.5\tau_H}{1+(\omega_H\tau_H)^2}+\frac{3\tau_H}{1+\{(1+\gamma_V/\gamma_H)\omega_H\tau_H\}^2}\right]\right\} dS, \tag{2}$$

where $F(S)$ is a distribution function of correlation times.

$$F(S) = \frac{1}{\beta_1\sqrt{\pi}}\exp\left(-\frac{S^2}{\beta_1^2}\right), \tag{3}$$

$$S = \ln\frac{\tau_H}{\tau_{mH}}, \tag{4}$$

$$\beta_1^2 = \beta_0^2 + \left(\frac{\beta_Q}{RT}\right)^2, \tag{5}$$

and

$$\tau_{mH} = \tau_{0H}\exp\left(\frac{E_H}{RT}\right). \tag{6}$$

Stable NMR active nuclei of V and Mo are $^{51}$V, $^{95}$Mo and $^{97}$Mo, respectively. The natural abundance of $^{51}$V is 99.8%. Contribution of Mo to $^1$H $T_1$ in $V_{1-x}Mo_xH_{0.68}$ ($x$ = 0.03, 0.05, 0.1) is considered to be negligible because the natural abundances of $^{95}$Mo and $^{97}$Mo are 15.7% and 9.5%, respectively, and their nuclear dipole moments are around 25% of $^{51}$V. The symbols of $\gamma_H$ and $\gamma_V$ are the gyromagnetic ratios of $^1$H and $^{51}$V spins, respectively. The symbol of $\omega_H$ is the angular resonance frequency of $^1$H, $E_H$ is the activation energy for the hydrogen diffusion, and $R$ is the gas constant. The symbol of $\tau_{mH}$ is the mean residence time and $\tau_{0H}$ is the mean residence time at the infinite temperature or the inverse of a frequency factor. The value of $\tau_{0H}$ was assumed to be $9\times10^{-14}$ s for the $O$ sites and $3\times10^{-14}$ s for the $T$ sites [29,30]. The symbols of $\beta_0$ and $\beta_Q$ are parameters defining the magnitude of the distributions of $\tau_{0H}$ and $E_H$, respectively. If $\beta_0$ = 0, only $E_H$ has a distribution. The symbol of $\beta_1$ is the total distribution parameter. The symbol of $f_1$ is a correction factor which reduces only the effective $M_{HV}$. The symbols of $M_{HH}$ and $M_{HV}$ are the second moments between $^1$H spins and between $^1$H and $^{51}$V spins, respectively:

$$M_{HH} = \frac{3}{5}\gamma_H^4\hbar^2 I_H(I_H+1)\sum_i r_i^{-6}, \tag{7}$$

and

$$M_{HV} = \frac{4}{15}\gamma_H^2\gamma_V^2\hbar^2 I_V(I_V+1)\sum_j r_j^{-6}. \tag{8}$$

The symbol of $\hbar$ is Plank constant. The symbols of $r_i$ and $r_j$ are the distances between $^1$H spins and between $^1$H and $^{51}$V spins, respectively, and those values were calculated from the BCT lattice whose lattice parameter were determined by XRD. The symbols of $I_H$ and $I_V$ are the nuclear spin quantum numbers of $^1$H and $^{51}$V, which are 1/2 and 7/2, respectively.

## 4. Results and discussion

The XRD measurements showed that $V_{1-x}Mo_x$ ($x$ = 0.03, 0.05, 0.1) before hydrogenation had a BCC structure. Their lattice parameters were calculated from the peak positions. Fig. 1(a) and (b) shows lattice parameters and unit cell volume of $V_{1-x}Mo_x$ ($x$ = 0.03, 0.05, 0.1) in comparison with pure V [31]. The BCC lattice expanded with increase in the Mo content, $x$, because Mo has a larger atomic radius than V [31].

Fig. 2 shows the $P$–$C$ isotherms of the $V_{1-x}Mo_x$–$H_2$ ($x$ = 0, 0.03, 0.05, 0.1) systems. The absorption and desorption isotherms of the V–$H_2$ system showed plateau regions under hydrogen pressures of 0.6 and 0.3 MPa at 303 K, respectively. The plateau regions are attributed to coexistence of the β and γ phases. The hydrogen content, H/V, under 7 MPa was 1.95. The equilibrium pressure of the plateau region increased with increase in $x$ from 0 to 0.05. For $x$ = 0.1 the plateau region was not found below the hydrogen pressure of 9 MPa at 303 K, but it was observed at 243 K as shown in Fig. 2. The hydrogen content, $H/V_{0.9}Mo_{0.1}$, under 5 MPa at 243 K was 1.74 which was 11% below that for $x$ = 0 at 303 K.

The XRD patterns of $V_{1-x}Mo_xH_{0.68}$ ($x$ = 0, 0.03, 0.05, 0.1) indicated that all the hydrides were the β phase with a BCT structure. The lattice parameter, $a$ increased and $c$ decreased with increase in $x$, as shown in Fig. 1(a). The unit cell volume was around 0.0308 nm$^3$ in the region of $0 \le x \le 0.05$ shown in Fig. 1(b), but that

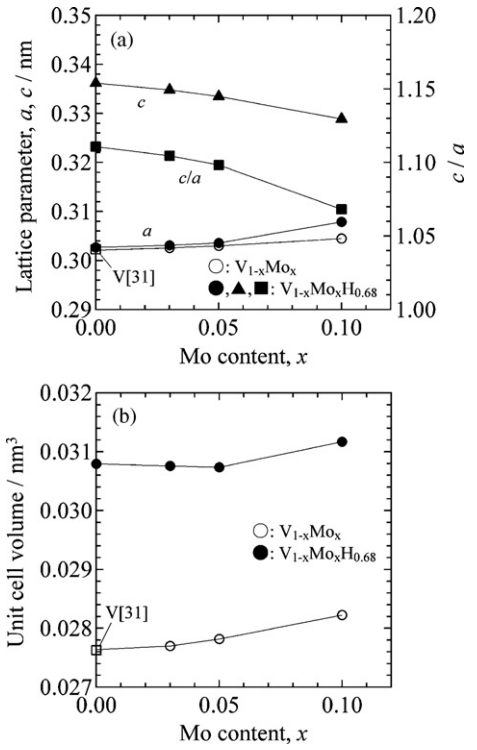


**Fig. 1.** (a) Lattice parameters and (b) unit cell volume of V [31], $V_{1-x}Mo_x$ and $V_{1-x}Mo_xH_{0.68}$ ($x$ = 0, 0.03, 0.05, 0.1).

was increased to 0.0312 $nm^3$ by increase in $x$ from 0.05 to 0.1. The BCC lattice of V expands along the $c$-axis by the phase transformation from the α phase to the β phase [13]. It is known that hydrogen occupation of the $O_z$ sites leads to this anisotropic expansion [13]. The value of $c/a$ decreased with increase in $x$, which indicates that addition of Mo reduces the anisotropy of the lattice expansion from the α phase to the β phase. This suggests that Mo addition affects hydrogen sites in the β phase of V–H.

Fig. 3 shows $^1$H NMR spectra of $V_{1-x}Mo_xH_{0.68}$ ($x$ = 0, 0.03, 0.05, 0.1) measured at 200.13 MHz and 138 K. The line width of the spectra is affected mainly by dipole–dipole interactions between $^1$H spins and between $^1$H and $^{51}$V spins because the contents of $^{95}$Mo and $^{97}$Mo are significantly lower than those of $^1$H and $^{51}$V. The line width of $V_{0.9}Mo_{0.1}H_{0.68}$ was smaller than the others. The temperature dependence of the $^1$H NMR spectra of $VH_{0.68}$ measured at 200.13 MHz is shown in Fig. 4. The line width decreased with increase in temperature from 138 to 240 K. This is due to motional

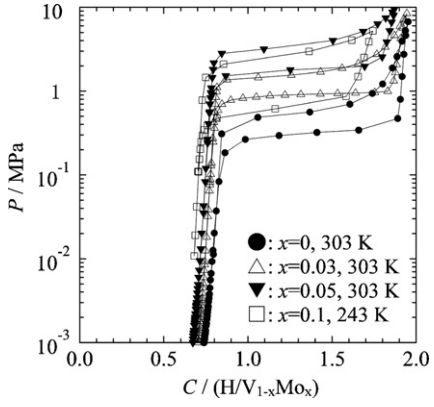


**Fig. 2.** Pressure–composition isotherms of the $V_{1-x}Mo_x$–$H_2$ systems; $x$ = 0, 0.03 and 0.05 at 303 K and $x$ = 0.1 at 243 K.

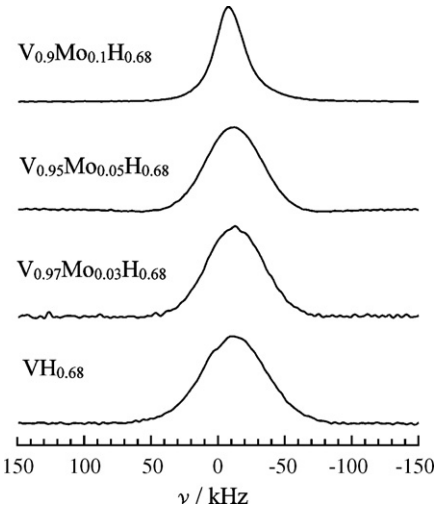


**Fig. 3.** $^1$H NMR spectra of $V_{1-x}Mo_xH_{0.68}$ ($x$ = 0, 0.03, 0.05, 0.1) measured at 200.13 MHz and 138 K.

narrowing by increasing hydrogen mobility on the $O$ sites. The reduction in the line width with increase in temperature was also observed for $x$ = 0.03, 0.05 and 0.1. The temperature dependence of the full-width at half maximum (FWHM) of the signal of the four hydrides measured at 200.13 MHz is plotted in Fig. 5. The FWHM was almost constant above room temperature. The motional narrowing was observed below 240 K other than for $V_{0.9}Mo_{0.1}H_{0.68}$. The FWHM of $V_{0.9}Mo_{0.1}H_{0.68}$ remained small even below 240 K. This indicates that hydrogen mobility in $V_{0.9}Mo_{0.1}H_{0.68}$ is higher than that in the others in the lower temperature range.

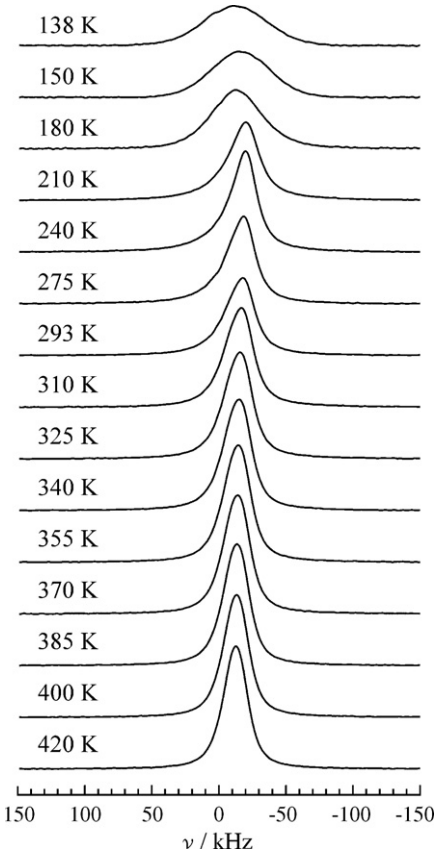


**Fig. 4.** Temperature dependence of $^1$H NMR spectra of $VH_{0.68}$ measured at 200.13 MHz.

**Table 1**
$^1$H Korringa constants and parameters for hydrogen diffusion in $V_{1-x}Mo_xH_{0.68}$ ($x$ = 0, 0.03, 0.05, 0.1).

| | $T_{1e}T$/s K | Site | $\tau_{0H}$/s | $E_H$/kJ mol$^{-1}$ | $\beta_Q$/kJ mol$^{-1}$ | $\beta_0$ | $f_1$ |
|---|---|---|---|---|---|---|---|
| $VH_{0.68}$ | 185 | *O* | $9\times10^{-14}$ | 25.7 | 2.8 | 0 | 0.69 |
| $V_{0.97}Mo_{0.03}H_{0.68}$ | 220 | *O* | $9\times10^{-14}$ | 26.0 | 3.6 | 0 | 0.66 |
| $V_{0.95}Mo_{0.05}H_{0.68}$ | 230 | *O* | $9\times10^{-14}$ | 25.4 | 3.6 | 0 | 0.60 |
| $V_{0.9}Mo_{0.1}H_{0.68}$ | 250 | *O* | $9\times10^{-14}$ | 23.2 | 3.6 | 0 | 0.38 |
| | | *T* | $3\times10^{-14}$ | 17 | 3.0 | 0 | 0.13 |

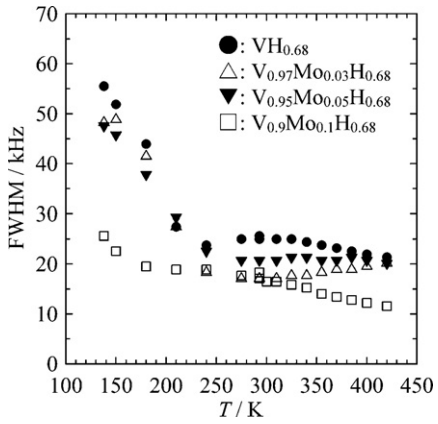


**Fig. 5.** Full-width at half maximum of $^1$H NMR signal of $V_{1-x}Mo_xH_{0.68}$ ($x$ = 0, 0.03, 0.05, 0.1) measured at 200.13 MHz.

Fig. 6(a)–(d) shows the temperature dependence of $^1$H spin-lattice relaxation time, $T_1$, in $V_{1-x}Mo_xH_{0.68}$ ($x$ = 0, 0.03, 0.05, 0.1) measured at 19.65 and 200.13 MHz. The value of $T_1$ at 19.65 MHz had a minimum at 250–310 K. The temperature for the minimum of $T_1$ shifted to a higher temperature with increase in the measurement frequency from 19.65 to 200.13 MHz. This is due to increase in hydrogen mobility at a higher temperature because the measurement frequency corresponds to the jump frequency of hydrogen atoms at the temperature for the minimum of $T_1$. The minimum value of $T_1$ was proportional to the measurement frequency because of $\omega_H\tau_H \approx 1$ in Eq. (2). With increase in $x$ the temperature for the minimum of $T_1$ shifted to a lower temperature. This indicates that addition of Mo makes hydrogen mobility higher. In addition, for $x$ = 0.1 shown in Fig. 6(d), the second component of $T_1$ appeared on the lower temperature side.

The temperature dependence of $T_1$ was fitted by Eqs. (1) and (2) and the fitting curves were shown in Fig. 6(a)–(d). For $x$ = 0, 0.03 and 0.05 the temperature dependence of $T_1$ was described by a single component in Fig. 6(a)–(c). This component was due to the contribution of hydrogen on the *O* sites because hydrogen atoms occupy the *O* sites in the β phase of V–H [13]. For $x$ = 0.1 the temperature dependence of $T_1$ showed the second component on the lower temperature side in Fig. 6(d), which is due to the contribution of hydrogen mobility between the *T* sites. Hayashi et al. have reported that the component of $T_1$ for the *T* sites was found on the lower temperature side compared to that for the *O* sites [27,30]. The component for the *O* sites on the higher temperature

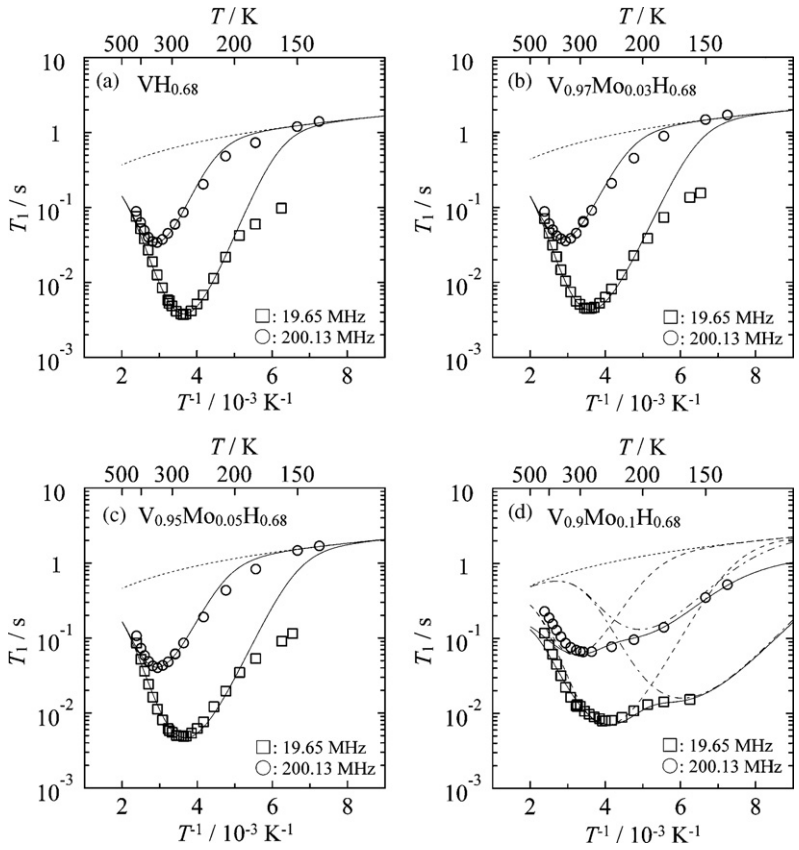


**Fig. 6.** $^1$H spin-lattice relaxation times in $V_{1-x}Mo_xH_{0.68}$ ($x$ = (a) 0, (b) 0.03, (c) 0.05, (d) 0.1) at 19.65 and 200.13 MHz and their simulated results indicated by the solid lines. The dotted lines indicate the contribution of conduction electrons. The chain lines in (d) indicate the components for the *O* and *T* sites.

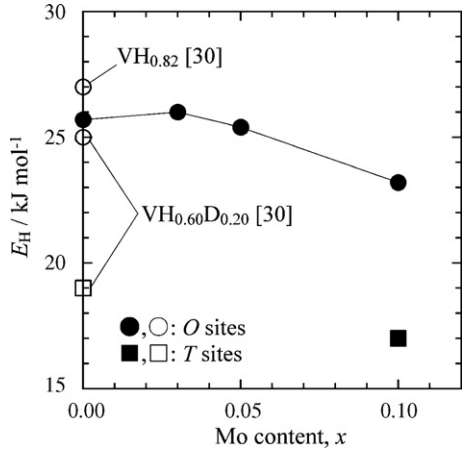


**Fig. 7.** Activation energy for hydrogen diffusion in $V_{1-x}Mo_xH_{0.68}$ ($x$ = 0, 0.03, 0.05, 0.1), $VH_{0.82}$ [30] and $VH_{0.60}D_{0.20}$ [30].

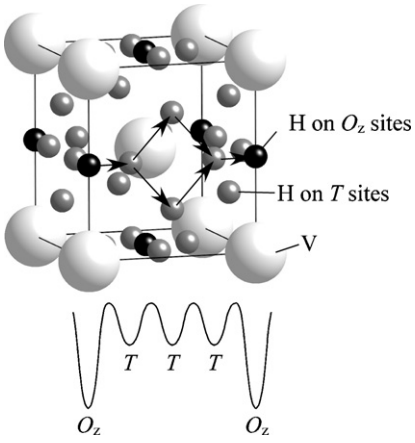


**Fig. 8.** Schematic drawing of diffusion paths of a hydrogen atom in the β phase of V–H and the potential energy along the paths [23].

side is due to the contribution of hydrogen mobility on the *T* and *O* sites. The activation energy for the hydrogen diffusion, $E_H$, in each hydride was evaluated. Table 1 lists the parameters obtained from the fitting of $T_1$. The value of $f_1$ for the *O* and *T* sites for $x$ = 0.1 was smaller than that for the *O* sites for the other three chemical compositions because the temperature dependence of $T_1$ for $x$ = 0.1 was divided into the two components for the *O* and *T* sites. The value of $E_H$ in $VH_{0.68}$ was 25.7 kJ mol$^{-1}$, which agreed well with that of 27.0 kJ mol$^{-1}$ reported in $VH_{0.82}$ [30]. Fukai and Kazama have reported the dependence of $E_H$ on the hydrogen content in the β phase of V–H [23]. The value of $E_H$ for the *O* sites was not changed by the hydrogen content above H/V ≈ 0.68 [23]. It is reasonable that obvious difference in $E_H$ between $VH_{0.68}$ prepared in the present work and $VH_{0.82}$ [30] is not found.

Fig. 7 shows the dependence of $E_H$ on the Mo content, $x$. The value of $E_H$ for the *O* sites was 25.7 kJ mol$^{-1}$ for $x$ = 0. The $E_H$ was almost constant between $x$ = 0 and 0.05 but that decreased to 23.2 kJ mol$^{-1}$ by increase in $x$ from 0.05 to 0.1. The $E_H$ was evaluated not only for the *O* sites but also for the *T* sites for $x$ = 0.1. The value of $E_H$ for the *T* sites was 17 kJ mol$^{-1}$, which was lower than that for the *O* sites. To our knowledge, neither hydrogen occupation of the *T* sites nor $E_H$ for the *T* sites in the β phase of V–H has not been reported. Hayashi et al. have reported that hydrogen and deuterium atoms occupy both the *O* and *T* sites in $VH_{0.60}D_{0.20}$ with a BCT structure and those on the *T* sites diffuse faster than those on the *O* sites [27,30]. The values of $E_H$ in $VH_{0.60}D_{0.20}$ have been estimated to be 25.0 kJ mol$^{-1}$ for the *O* sites and 19.0 kJ mol$^{-1}$ for the *T* sites [30]. On the other hand, Fukai and Kazama have reported the diffusion paths of a hydrogen atom in the β phase of V–H [23]. Fig. 8 shows the schematic drawing of the diffusion paths modified from their report [23]. A hydrogen atom occupying one of the $O_z$ sites migrates to another $O_z$ site through three *T* sites in succession. It is suggested that the residence time of hydrogen on the *O* sites is significantly longer than that on the *T* sites with decrease in temperature because the $E_H$ for the *O* sites is higher than that for the *T* sites.

The mean residence time of hydrogen, $\tau_{mH}$, can be calculated using Eq. (6) with $E_H$ for each site. The temperature dependence of $\tau_{mH}$ on the *O* sites in $VH_{0.68}$, on the *T* sites in $VH_{0.60}D_{0.20}$ [30] and on the *O* and *T* sites in $V_{0.9}Mo_{0.1}H_{0.68}$ is shown in Fig. 9. The value of $\tau_{mH}$ increased with decrease in temperature. The increase in $\tau_{mH}$ corresponds to decreasing hydrogen mobility. The $\tau_{mH}$ on the *O* sites was longer than that on the *T* sites. This indicates that hydrogen atoms on the *T* sites diffuse faster than those on the *O* sites. The $\tau_{mH}$ on the *O* and *T* sites in $V_{0.9}Mo_{0.1}H_{0.68}$ was shorter than that on the *O* sites in $VH_{0.68}$ and that on the *T* sites in $VH_{0.60}D_{0.20}$ [30], respectively. For $x$ = 0, 0.03 and 0.05 the temperature dependence of $T_1$ was described by the component of the *O* sites in Fig. 6(a)–(c). The component of the *T* sites was not clearly observed for them but the value of $T_1$ especially at 19.65 MHz was slightly smaller than each fitting curve below 200 K, where the component of the *T* sites was found for $x$ = 0.1 in Fig. 6(d). This suggests that a small amount of hydrogen atoms occupy the *T* sites for $x$ = 0, 0.03 and 0.05 and the hydrogen occupancy of the *T* sites for $x$ = 0.1 is significantly higher than the other three chemical compositions.

The anisotropic lattice expansion from the α phase to the β phase is accompanied by change in site occupation of hydrogen [13]. Hydrogen atoms on the *T* sites shift to the $O_z$ sites with increase in $c/a$ and those on the $O_z$ sites are the most stable at $c/a \approx 1.1$ [32]. The value of $c/a$ obtained for the β phase of $V_{1-x}Mo_xH_{0.68}$ was 1.10–1.11 for $x$ = 0, 0.03 and 0.05, and 1.07 for $x$ = 0.1. The difference in $c/a$ is attributed to increase in hydrogen occupancy of the *T* sites. Mo addition promoted the shift in hydrogen occupation from the $O_z$ sites to the *T* sites by reducing the size of the $O_z$ site. Kamegawa et al. have reported that Mo added Ti–Cr alloys with a BCC structure formed the monohydride phase with a BCC structure [9]. It seems that this isotropic lattice expansion by hydrogenation is also due to low hydrogen occupancy of the $O_z$ site compared to pure V.

It has been reported that addition of Mo to BCC metals affects the site occupation of hydrogen in the hydrogen solid solution phase (α phase). The hydrogen diffusion was affected by change in the site occupation. Nb metal forms the α phase with a BCC structure and hydrogen atoms occupy the *T* sites [13], which is similar to

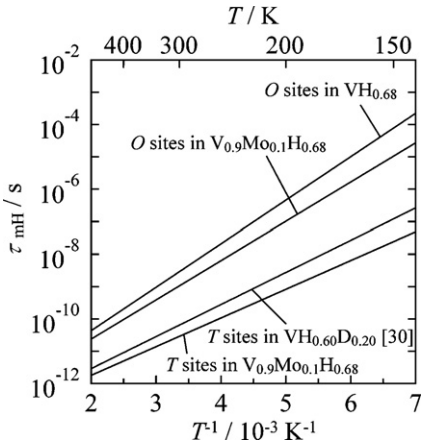


**Fig. 9.** Mean residence times on the *O* sites in $VH_{0.68}$, on the *T* sites in $VH_{0.60}D_{0.20}$ [30] and on the *O* and *T* sites in $V_{0.9}Mo_{0.1}H_{0.68}$.

the V–$H_2$ system. Yagi et al. have reported that hydrogen atoms shift to Mo atoms below $x = 0.1$ in the α phase of $Nb_{1-x}Mo_x$–H and that those occupy not only the *T* sites but also the *O* sites above $x = 0.2$ [33,34]. On the other hand, Tanaka and Kimura have determined the diffusion coefficient of hydrogen, $D_H$, in the α phase of V–H and $V_{0.99}Mo_{0.01}$–H by means of the electric resistivity method [18]. The value of $D_H$ at 273 K was slightly reduced by addition of Mo. Mazzolai has determined the $D_H$ and $E_H$ in the α phase of $Ti_xCr_{0.975-x}Mo_{0.025}$–H ($x = 0.515, 0.545$) by means of the absorption method [35]. The value of $E_H$ was increased by addition of Mo. He explained that it was due to attractive interaction between hydrogen and Mo atoms. On the contrary, for the β phase of $V_{1-x}Mo_x$–H in the present work, Mo addition affects the site occupation of hydrogen, *i.e.*, hydrogen atoms shift from the $O_z$ sites to the *T* sites in $V_{0.9}Mo_{0.1}H_{0.68}$. Hydrogen atoms in $V_{0.9}Mo_{0.1}H_{0.68}$ can diffuse faster than those in $VH_{0.68}$ because the $\tau_{mH}$ on the *O* and *T* sites in $V_{0.9}Mo_{0.1}H_{0.68}$ was shorter than that on the *O* sites in $VH_{0.68}$.

## 5. Conclusions

Hydrogen atoms occupied mainly the *O* sites in the β phase of $V_{1-x}Mo_xH_{0.68}$ from $x = 0$ to 0.05. The activation energy for the hydrogen diffusion for the *O* sites decreased from $x = 0.05$ to 0.1. Hydrogen atoms occupy not only the *O* sites but also the *T* sites in $V_{0.9}Mo_{0.1}H_{0.68}$. Shift of hydrogen occupation from the *O* sites to the *T* sites accompanied the reduction in the axis ratio of the BCT lattice, *c*/*a*. The activation energy for the hydrogen diffusion for the *T* sites was lower than that for the *O* sites. In conclusion, Mo addition affected the site occupation of hydrogen and enhanced the diffusion of hydrogen in the β phase of V–H.

## Acknowledgements

The authors would like to thank Dr. R. Chiba and Dr. Y. Suzuki of National Institute of Advanced Industrial Science and Technology (AIST) for their technical advices on NMR. This work was supported by The New Energy and Industrial Technology Development Organization (NEDO) under "Advanced Fundamental Research on Hydrogen Storage Materials (Hydro-Star)".

## References

[1] L. Schlapbach, A. Züttel, Nature 414 (2001) 353.
[2] L. Schlapbach, Nature 460 (2009) 809.
[3] N. Takeichi, H. Senoh, T. Yokota, H. Tsuruta, K. Hamada, H.T. Takeshita, H. Tanaka, T. Kiyobayashi, T. Takano, N. Kuriyama, Int. J. Hydrogen Energy 28 (2003) 1121.
[4] D. Mori, K. Hirose, Int. J. Hydrogen Energy 34 (2009) 4569.
[5] H. Iba, E. Akiba, J. Alloys Compd. 253–254 (1997) 21.
[6] E. Akiba, H. Iba, Intermetallics 6 (1998) 461.
[7] D. Mori, N. Haraikawa, T. Shinozawa, T. Matsunaga, K. Toh, K. Fujita, Trans. Japan Soc. Mech. Eng 73 (2007) 1236 (in Japanese).
[8] T. Matsunaga, M. Kon, K. Washio, T. Shinozawa, M. Ishikiriyama, Int. J. Hydrogen Energy 34 (2009) 1458.
[9] A. Kamegawa, K. Shirasaki, T. Tamura, T. Kuriiwa, H. Takamura, M. Okada, Mater. Trans. 43 (2002) 470.
[10] A. Kamegawa, T. Tamura, H. Takamura, M. Okada, J. Alloys Compd. 356–357 (2003) 447.
[11] K. Kubo, H. Itoh, T. Takahashi, T. Ebisawa, T. Kabutomori, Y. Nakamura, E. Akiba, J. Alloys Compd. 356–357 (2003) 452.
[12] K. Iwase, Y. Nakamura, K. Mori, S. Harjo, T. Ishigaki, T. Kamiyama, E. Akiba, J. Alloys Compd. 404–406 (2005) 99.
[13] T. Shober, H. Wenzl, in: G. Alefeld, J. Völkl (Eds.), Hydrogen in Metals, vol. II, Springer-Verlag, Berlin, 1978, p. 11.
[14] R. Cantelli, F.M. Mazzolai, M. Nuovo, J. Phys. Chem. Solids 31 (1970) 1811.
[15] G. Schaumann, J. Völkl, G. Alefeld, Phys. Stat. Sol. 42 (1970) 401.
[16] U. Freudenberg, J. Völkl, J. Bressers, G. Alefeld, Scripta Metall. 12 (1978) 165.
[17] R.C. Brouwer, J. Rector, N. Koeman, R. Griessen, Phys. Rev. B 40 (1989) 3546.
[18] S. Tanaka, H. Kimura, Mater. Trans. JIM 20 (1979) 647.
[19] D.J. Pine, R.M. Cotts, Phys. Rev. B 28 (1983) 641.
[20] T. Eguchi, S. Morozumi, J. Jpn. Inst. Met. 41 (1977) 795 (in Japanese).
[21] K. Takata, T. Suzuki, Mater. Sci. Eng. A 163 (1993) 91.
[22] N. Fujimura, K. Asano, Y. Iijima, to be submitted.
[23] Y. Fukai, S. Kazama, Acta Metall. 25 (1977) 59.
[24] R.C. Bowman Jr., A. Attalla, W.E. Tadlock, D.B. Sullenger, R.L. Yauger, Scripta Metall. 16 (1982) 933.
[25] R.C. Bowman Jr., A. Attalla, B.D. Craft, Scripta Metall. 17 (1983) 937.
[26] T. Ueda, S. Hayashi, J. Alloys Compd. 231 (1995) 226.
[27] B. Bandyopadhyay, S. Hayashi, Phys. Rev. B 60 (1999) 10302.
[28] N. Bloembergen, E.M. Purcell, R.V. Pound, Phys. Rev. 73 (1948) 679.
[29] S. Hayashi, J. Solid State Chem. 170 (2003) 82.
[30] S. Hayashi, J. Phys. Chem. Solids 64 (2003) 2227.
[31] Metal Databook Ver. 3, Japan Institute of Metals, 1993 (in Japanese).
[32] Y. Fukai, The Metal-Hydrogen System, Basic Bulk Properties, 2nd ed., Springer-Verlag, Berlin, Heidelberg, 2005, p. 244.
[33] E. Yagi, S. Koike, T. Matsumoto, T. Urai, N. Tajima, K. Ogiwara, Phys. Rev. B 66 (2002) 024206.
[34] E. Yagi, ISIJ Int. 43 (2003) 505.
[35] G. Mazzolai, Int. J. Hydrogen Energy 33 (2008) 7116.